Chinese Journal of Information Fusion
http://dx.doi.org/10.62762/CJIF.2025.519610

RESEARCH ARTICLE

A Track Splitting Determination Method for Elliptical Extended Targets Based on Spatio Temporal Similarity

Jiashi Shen[1], **Chaoqun Yang**[1,2,*], **Lidong He**[3] and **Xianghui Cao**[1]

[1] School of Automation, Southeast University, Nanjing 210096, China
[2] Key Laboratory of Measurement and Control of Complex Systems of Engineering, Nanjing 210096, China
[3] School of Automation, Nanjing University of Science and Technology, Nanjing 210094, China

Abstract

Extended target tracking in occlusion scenarios often suffers from split errors due to sensor limitations and complex target interactions, leading to degraded tracking performance for autonomous vehicles and surveillance systems. To address this issue, in this paper, we propose a Gaussian Wasserstein distance-enhanced spatio-temporal similarity method for split error correction. We first analyze the spatio-temporal characteristics of split extended targets and model their geometric uncertainties via elliptical Gaussian distributions. Then, we integrate the Gaussian Wasserstein distance into the clue-aware trajectory similarity calculation framework to simultaneously capture positional and shape discrepancies, and designs an adaptive validation gate mechanism to dynamically adjust the threshold for track splitting, enabling accurate determination and fusion of split targets. Finally, simulation experiments are conducted to demonstrate the effectiveness of the proposed method.

Keywords: extended target tracking, target splitting, gaussian wasserstein distance, spatiotemporal trajectories, error correction.

Academic Editor:
Jun Liu

Submitted: 27 March 2025
Accepted: 29 May 2025
Published: 25 June 2025

Vol. 2, **No.** 2, 2025.
10.62762/CJIF.2025.519610

***Corresponding author:**
Chaoqun Yang
ycq@seu.edu.cn

1 Introduction

Currently, with the deep and extensive popularization of high-precision sensors in cutting-edge fields such as autonomous driving, robot navigation, and security monitoring, extended target tracking (ETT) technology has emerged as a new research hotspot [1, 2]. Compared to the issue of traditional point target tracking, extended target tracking encompasses multiple information dimensions such as position, shape and velocity, which undoubtedly poses more stringent requirements on the accuracy and complexity of tracking algorithms [3].

To achieve effective tracking of extended targets, numerical methods have been addressed. For example, Granstrom et al. [4] introduced probability hypothesis density (PHD) filter and cardinalized probability hypothesis density (CPHD) filter into the ETT field. Then two measurement set partitioning methods [5] were added into the filters in [4].

Citation
Shen, J., Yang, C., He, L., & Cao, X. (2025). A Track Splitting Determination Method for Elliptical Extended Targets Based on Spatio Temporal Similarity. *Chinese Journal of Information Fusion*, 2(2), 171–181.

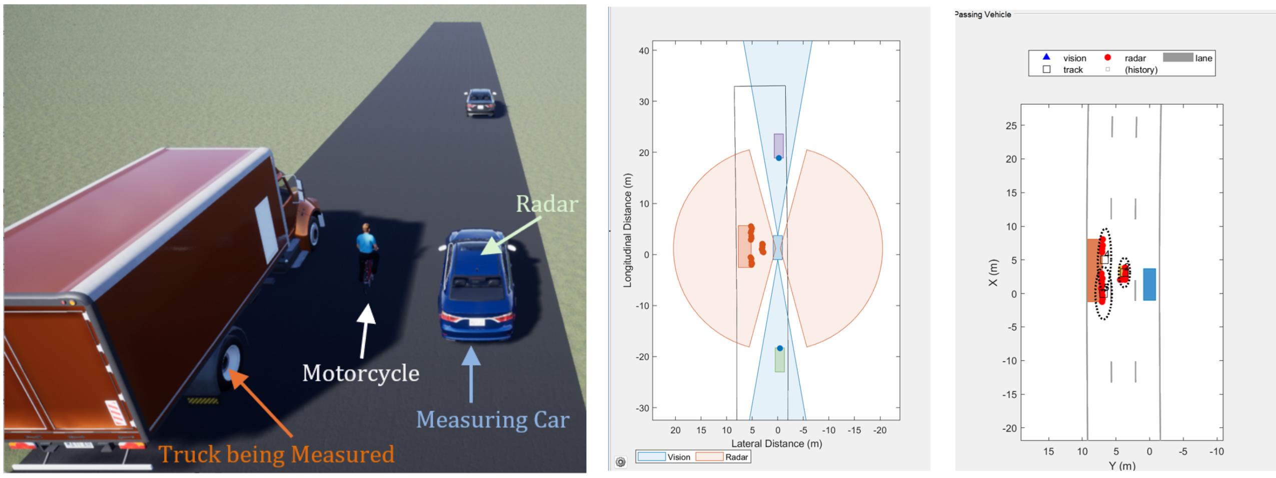

(a) Simulation scene (b) Sensor distribution (c) Tracking results

Figure 1. An autonomous driving scenario: A car with radar and vision sensors is driving on a highway. Due to the presence of occlusion, the truck is mistakenly recognized as two targets, resulting in a split situation.

Additionally, Habtemariam et al. [6] integrated the measurement unit generation strategy with joint probability data association (JPDA), thereby proposed the multi-detection joint probability data association (MD-JPDA) method. Zhang et al. [7] introduced the cardinality balanced multi-target multi-Bernoulli (CBMeMBer) algorithm and successfully conducted the ETT task. In [8], the generalized labeled multi-Bernoulli (GLMB) and Gamma Gaussian inverse Wishart (GGIW) distributions were used to precisely model the states and extension characteristics of multiple extended targets. Then, the GGIW Poisson model was ingeniously embedded into the multi-Bernoulli filter to cope with the issue of multi-extended target tracking [9]. Recently, an approach based on irregular probability distributions has also been proposed to cope with this issue [10].

However, when extended targets are occluded or densely distributed, due to their non-point nature and their complex interaction patterns in dynamic environments, the methods mentioned above are prone to trigger the challenging problem of target splitting or merging during actual operation. For example, in Figure 1(a), the radar of the car is occluded by a motorcycle, resulting in the truck being identified as two split targets, as shown in Figure 1(c). To cope with this problem, the key lies in accurately distinguishing whether the target has truly split or it is merely false alarm.

A few related works have been proposed to address the above problem. For visual targets, [11] detected target splitting positions and segments trajectories by stacking temporal dilated convolution blocks and an adaptive Gaussian smoothing label strategy. For missile targets, [12] constructed a mathematical model for splitting event detection and tracking within the joint integrated probabilistic data association (JIPDA) framework, achieving point target splitting determination and tracking through probability calculations of splitting events. [13] optimized the de-correlation time of group targets using Pareto analysis based on the interactive multiple model-unscented Kalman filter (IMM-UKF) framework, which essentially performs data association on point targets within group targets. It is important to note that these methods only utilize the position data of point targets. Directly applying them in extended target tracking scenarios cannot fully leverage the extended information of targets, leading to poor performance. To the best of our knowledge, there has been no work addressing the problem of splitting and merging of extended targets so far.

Motivated by this, we aim to make use of extended information and achieve accurate determination and fusion of split targets. To this end, we first analyze the extended target splitting problem with PHD-based filters, and then present the similarity of the track feature of extended targets. Next, we expand spatio-temporal [14] based clue-aware trajectory similarity (CATS) method to the ETT issue by integrating the Gaussian Wasserstein (GW) distance. Subsequently, we develop an extended target split error correction algorithm.

In summary, the main contribution of this paper is the proposed method that can solve the splitting problem of extended targets by using the spatio-temporal trajectories and extended information of extended targets. Furthermore, as far as we know, the method presented in this paper is the first work to deal with the issue of the split of extended target.

The organization of this paper is as follows. Section 2 describes the problem of extended target splitting in detail. Section 3 analyzes the split tracks' information. Section 4 elaborates on the proposed splitting determination method. Section 5 builds a simulation scenario to verify the effectiveness of proposed method. Section 6 summarizes the entire paper.

2 Problem Formulation

2.1 Extended Target Modeling

In this paper, a two dimensional ellipse is used to represent an extended target. The extended target state ξ is defined as a triple:

$$\xi \triangleq (\gamma, \mathbf{x}, X) \tag{1}$$

where $\gamma > 0$ represents the measurement rate, $\mathbf{x} = [p, v, \omega]^T \in \mathbb{R}^5$ represents the kinematic state, which includes its position $p \in \mathbb{R}^2$, velocity $v \in \mathbb{R}^2$ and turn-rate $\omega \in \mathbb{R}^1$ that characterizes the rate of alteration in the direction of the velocity vector v, where $\mathbb{R}^n$ denotes the set of real n vectors. X represents the extended geometric information that includes the shape, size and direction of the ellipse extended target and

$$X = R \cdot D \cdot R^T \triangleq \begin{bmatrix} (r_1)^2 & \sigma \\ \sigma & (r_2)^2 \end{bmatrix} \in \mathbb{S}^2_{++} \tag{2}$$

where $\mathbb{S}^n_{++}$ denotes the set of symmetric positive definite $n \times n$ matrices. The rotation matrix R and the diagonal matrix D are represented as follows:

$$R = \begin{bmatrix} \cos(\alpha) & -\sin(\alpha) \\ \sin(\alpha) & \cos(\alpha) \end{bmatrix} \quad D = \begin{bmatrix} (r_1)^2 & 0 \\ 0 & (r_2)^2 \end{bmatrix} \tag{3}$$

where α is the rotation angle of the ellipse, r_1 and r_2 are defined as the major/minor axes of the ellipse and σ controls the rotation.

2.2 Extended Target Tracking Method

PHD-based filters are widely used in the field of multiple extended target tracking, such as GGIW-PHD and GGIW-CPHD filters [15]. In order to formulate the problem of target splitting, we take PHD-based filter as the front-end process. Assume that GGIW-PHD filter [16] will output an extended target track set with labels. Specifically, at time step k, the track information obtained from the front-end tracker is represented as $T_k = \{T_k^l\}_{l=1}^L$, where L is the total number of tracks in the set. Each element T_k^l is defined as:

$$T_k^l = (t_k^l; \xi_k^l; A_k^l; l) \tag{4}$$

where l is the unique index (it is referred to as label in the following text) of each track, t_k^l denotes the extended target detection time, ξ_k^l denotes the extended target state, A_k^l denotes the "age" that target exists.

By grouping together the elements from different time steps with the same label l, we can obtain the track sequence arranged in chronological order:

$$T^l = \{T_k^l\}_{k=St}^{Tt} \tag{5}$$

where St and Tt denote the start and end time step of track l sequence. It should be noted that in this paper, track l sequence will be called "**track**" T^l and T_k^l will be called the "**element**" of track T^l.

2.3 The Objective of This Paper

Consider the automatic driving scenario shown in Figure 1. At time step k, in addition to the original surviving target track T^i with label i, there appears a new track T^j with label j, indicating the potential emergence of a new extended target. Now, there are three possibilities for this new track:

1. It is split from the long-existing track T^i, such as the truck in Figure 1, which is split into two targets.
2. It is a new track, such as the two-wheeled motorcycle in Figure 1.
3. False alarm. That is:

$$j = \begin{cases} i, & split \\ j, & newborn \\ \emptyset, & false\ alarm \end{cases} \tag{6}$$

The formulated problem is how to accurately judge which of the above three cases the new target state belongs to. Therefore, the goal of this paper is to propose an effective method to determine whether the extended object is split or not, and if it is split, then select an appropriate fusion method to fuse the two tracks.

3 Similarity Analysis of Track Feature

First of all, we will analyze the track feature of the split extended targets in this section.

As described above, an elliptic extended target information includes position p, detection time t and geometric information X. This elliptic can be interpreted as the following Gaussian distribution [17]:

$$\mathcal{ET} \triangleq \mathcal{N}(p, \mathbf{e_g}X) \tag{7}$$

where $\mathbf{e_g}$ is scaling factor relates to the tolerance region that is user-defined. In addition, due to the uncertainty of sensor measurement and data processing, the detection time can also be considered to obey the following Gaussian distribution:

$$\mathcal{NT} \triangleq \mathcal{N}(t, \mathbf{e_t}\triangle t^2) \tag{8}$$

where $\triangle t$ is time interval and $\mathbf{e_t}$ represents the scaling factor.

Suppose that track $T^{\cdot}$ which has already existed moves in a two-dimensional plane, after being tracked by the PHD-based filter, it splits into two tracks T^i and T^j with distribution sets $(\mathcal{ET}^i, \mathcal{NT}^i)$ and $(\mathcal{ET}^j, \mathcal{NT}^j)$, then their center sets (p^i, t^i) and (p^j, t^j) can be separately connected as a curve in a three-dimensional plane, as shown in Figure 2.

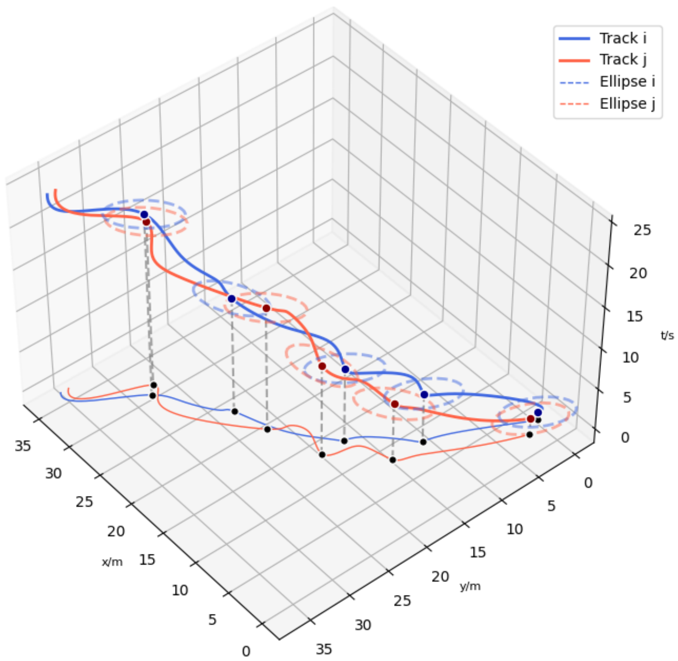

Figure 2. An illustration of spatio-temporal prism structure.

It can be observed that, influenced by various factors, there are deviations in the area where the two distributions should overlap, and the deviation shows the following characteristics: The deviations in detection time are highly random, but the deviations in spatial position are relatively fixed, and there are slight deviations in the rotation angle. Additionally, some measurement data are missing. Hence, if the two tracks are originated from the same track, they are actually a kind of spatio-temporal prism structure [18] with a range of uncertainty. Thus, we can use the similarity of historical track information to determine the split possibility of extended target.

In order to determine the split possibility, the clue-aware trajectory similarity (CATS) method based on spatial and temporal information in [19] is chosen. Its main idea is to find potential "matching points" on the two tracks when evaluating the spatial and temporal similarity. However, since it is inappropriate to use the center point to represent the extent of an ellipse, the direct application of the CATS method will result in unsatisfactory outcomes. Therefore, we propose a new method called GW-CATS to determine the splitting of extended targets, which will be elaborated in the next Section.

4 Extended Target Splitting Determination Method

Before introducing the determination method, we first introduce Gaussian Wasserstein distance [17].

For elements $T_a^i \in T^i$ and $T_b^j \in T^j$, they can construct two elliptical extended targets subjected to the following Gaussian distributions:

$$\begin{aligned} \mathcal{ET}_a^i &= \mathcal{N}(p_a^i, X_a^i) \\ \mathcal{ET}_b^j &= \mathcal{N}(p_b^j, X_b^j) \end{aligned} \tag{9}$$

The Gaussian Wasserstein distance between the two extended targets provides the similarity measure metric that is defined as:

$$d_{GW}(\mathcal{ET}_a^i, \mathcal{ET}_b^j) = \sqrt{\|p_a^i - p_b^j\|_2^2 + Tr\left(X_a^i + X_b^j - 2\sqrt{\sqrt{X_a^i}X_b^j\sqrt{X_a^i}}\right)} \tag{10}$$

where $Tr(\cdot)$ represents the trace operator.

This metric simultaneously captures positional offsets and quantifies the congruence between the two targets' shapes through their covariance matrices. In this article, $d_{GW}(\mathcal{ET}_a^i, \mathcal{ET}_b^j)$ will be represented by the shorthand notation $d_{GW}(T_a^i, T_b^j)$.

The main idea of the CATS method is to evaluate the spatial and temporal similarity of different tracks. The core workflow is as follows: First, temporal and spatial thresholds are set to filter elements contained in the two tracks, selecting element pairs from different tracks that are temporally and spatially close. Subsequently, the spatial distances between these element pairs are normalized to identify the most similar pairs. Lastly, the similarity between two tracks is computed as the average of all normalized similarity scores of their best-matching element pairs.

Since CATS handles point targets through Euclidean distance, it fails to account for extended target. Thus, we propose the GW-CATS method that addresses this limitation by incorporating geometric information, enabling a more reasonable use of extended information. The detailed implementation of the proposed method is as follows.

At time step k, suppose that the track information is obtained from the front-end tracker. Thereinto, T^j represents a newborn track and T^i represents an existing track. In order to calculate the similarity between track T^i and track T^j, the following four-step process is adopted as follows:

Step 1: Spatio-temporal Matching Elements Finding

Given a spatial threshold ϵ, a time threshold τ, two elements $T_b^j \in T^j$ and $T_a^i \in T^i$, if T_b^j and T_a^i satisfy the following conditions:

$$(1)\ |t_b^j - t_a^i| \leq \tau, \qquad (2)\ d_{GW}(T_b^j, T_a^i) \leq \epsilon,$$

then we call T_a^i is the spatio-temporal matching element of T_b^j and $\{T_a^i \rightarrow T_b^j\}$ is a spatio-temporal matching pair.

Similar to the CATS method, we set a time threshold ϵ and a space threshold τ to compensate for the uncertainty of target kinematics and sensor measurements. Due to the existence of extended target velocity information, After the determination of user-defined time threshold ϵ according to the actual situation, the spatial threshold τ can be calculated by the following method.

As shown in Figure 3, the initial center position of extended target T_b^j is set as p_b^j, its speed is v_b^j, and turning rate perpendicular to the direction of the velocity vector is w_b^j. After passing time τ, the center of the target $T(\tau)_b^j$ reaches the position $p(\tau)_b^j$. Since τ is relatively small, the target speed can be approximated as constant during the motion. Then,

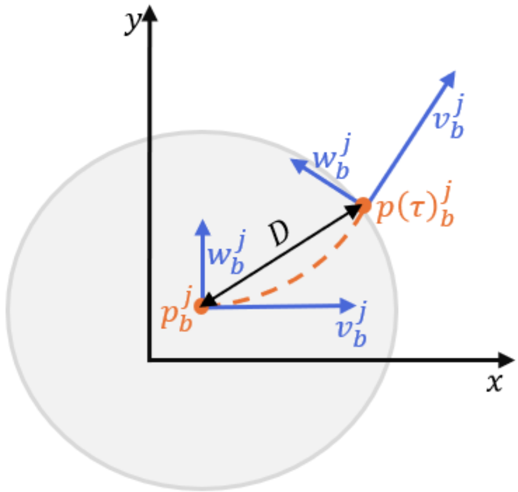

Figure 3. Geometric illustration of the spatial threshold.

the Euclidean distance D between point p_b^j and $p(\tau)_b^j$ can be expressed as:

$$D = ||p_b^j - p(\tau)_b^j||_2 = \begin{cases} \frac{2||v_b^j||_2}{w_b^j} sin(\frac{w_b^j \tau}{2}) & (w_b^j \neq 0) \\ ||v_b^j||_2 \times \tau & (w_b^j = 0) \end{cases} \tag{11}$$

where $||\cdot||_2$ denotes the 2-norm operator. Using D as the radius, a validation gate is constructed to filter spatially irrelevant elements, as shown in gray part in Figure 3. Since τ is relatively small, the elliptical rotation angle $\alpha = w\tau$ remains minimal. By neglecting rotational effects, we derive:

$$\epsilon = d_{GW}(T_b^j, T(\tau)_b^j) \approx D \tag{12}$$

The detailed derivation is provided in Appendix.

Step 2: Similarity Calculation of Matching Elements

For any elements in the reference track, the number of matching elements from other tracks may be zero, one, or multiple.

To distinguish matching elements and find the most similar matching pair, we quantify similarity scores through numerical normalization to the range [0,1], enabling optimal matching selection. Thus, the similarity of matching elements are calculated as follows [20] :

$$f_{\epsilon,\tau}(T_a^i \rightarrow T_b^j) = 1 - \frac{d_{GW}(T_b^j, T_a^i)}{\epsilon} \tag{13}$$

where T_a^i is a matching element of T_b^j and the value range of the function $f_\epsilon(T_a^i \rightarrow T_b^j)$ is limited in [0,1]. The closer the position and geometric information of two ellipses are, the larger this function value is, indicating greater similarity. If two extended targets are exactly the same, this function's value equals to 1. For brevity, $f_\epsilon(T_a^i \to T_b^j)$ will be abbreviated to $f^{ai\to bj}$.

Step 3: Best Matching Element Confirm

After similarity calculation, we can confirm the best matching element of T_b^j. Suppose that track T^i contains n elements, for $T_a^i \in T^i$, if:

$$f_{\epsilon,\tau}(T_a^i \to T_b^j) = \mathbf{Max}\{f_{\epsilon,\tau}(T_q^i \to T_b^j)\,|_{q=St}^{Tt}\} \tag{14}$$

then we call T_a^i the best matching element of T_b^j, where T_q^i represents any matching element of T_b^j in track T^i.

Best matching element pairs are defined as those that optimally capture the same kinematic characteristics. When two tracks are hypothesized to originate from the same physical target, our objective is to systematically identify these optimal element pairs, thereby enabling the subsequent processing step.

Step 4: Similarity Calculate of Two Tracks

Finally, after the above three steps, we obtain the best matching elements and matching values of each elements in track T^j. The inter-track similarity is determined by aggregating and averaging the normalized similarity scores across all matched element pairs. Thus, the spatio-temporal similarity of track T^i to track T^j is defined as:

$$S_{\epsilon,\tau}(T^i \to T^j) = \frac{1}{|T_j|} \times \sum_{b=St}^{Tt} f_{\epsilon,\tau}(T_a^i \to T_b^j) \tag{15}$$

where $|T^j|$ refers to the number of elements in T^j and T_a^i is the corresponding best matching element of T_b^j. For brevity, $S_{\epsilon,\tau}(T^i \to T^j)$ will be abbreviated to $S^{i\to j}$. In summary, a complete pseudocode implementation of the proposed method is provided in Algorithm 1.

For any newborn track T^j, its similarity score $S^{i\to j}$ with respect to each established independent track T^i can be systematically computed through Algorithm 1. By establishing a similarity threshold μ, we implement the following decision rule:

- If $S^{i\to j} > \mu$, tracks T^i and T^j are considered to represent the same physical target.

If two tracks are determined to be similar, the Monte Carlo Minimum Mean Gaussian Wasserstein (MC-MMGW) method can be used to fuse the information of the two extended targets. For the specific details of the fusion method, please refer to reference [21].

Algorithm 1: GW-CATS Method for track splitting determination

Input : Track T^i, T^j, Temporal threshold τ.
Output: Similarity score $S^{i\to j}$.

```
totalscore ← 0;
for b = 1 to length(T^j) do
    bestscore ← 0;
    Calculate D via (11);
    ϵ ← D;
    // Search candidate track elements
    for a = 1 to length(T^i) do
        if abs(T^i(a).time − T^j(b).time) > τ then
            Continue;
        end
        d ← d_GW(T^i(a), T^j(b));
        if d > ϵ then
            Continue;
        end
        // Update best matching score
        f^{ai→bj} ← 1 − d/ϵ, see (13);
        if f^{ai→bj} > bestscore then
            bestscore ← f^{ai→bj};
        end
    end
    totalscore ← totalscore + bestscore;
end
S^{i→j} ← totalscore / length(T^j);
return S^{i→j}
```

5 Numerical Experiments

In this section, we set a highway autonomous driving simulation scenario to evaluate the proposed GW-CATS method. We used the optimal sub-pattern assignment (OSPA) [22] and generalized optimal sub-pattern assignment (GOSPA) [23] as evaluation metric to Verify the effectiveness of the proposed GW-CATS method.

5.1 Simulation Scene Settings

Given $k = 136$ time steps, $t = 13.6s$ in total, we first set up the simulation scenario. The scenario is set in two-dimensional three-lane highway with lane width 3.5 m. The road centerline coordinates is [0 0 ; 50 0 ; 100 0 ; 250 20 ; 400 35]m. There are a total of five vehicles on the highway, and they all travel along the corresponding lane. Target parameters are listed in Table 1.

Specifically, target 4 represents a motorcycle, target 1 is a truck, Target 2 and 3 are standard vehicles. The RadarCar is an autonomous vehicle equipped with

Table 1. Target parameters.

Parameter	Dimensions (m^2)	Velocity (m/s)	Lifetime (s)
RadarCar	4.7×1.8	$25-\frac{t}{20}$	0.1-13.6
Target 1	4.7×1.8	25	0.1-13.6
Target 2	2.0×1.0	24	0.2-13.6
Target 3	4.7×1.8	26	0.3-13.6
Target 4	9.3×2.2	$35-\frac{t^2}{142}$	0.1-13.6

four radars, and radar parameters are listed below:

- Left/Right radars: 160° detection angle, 30 m range.
- Front/rear radars: 30° detection angle, 50 m range.
- Detection probability $P_d = 0.9$.
- False alarm rate $\lambda_{fa} = 1 \times 10^{-6}$.
- Clutter intensity $\lambda_{ck} = 8$ (Poisson point process distribution).

The GGIW-PHD filter is used to track these targets, its corresponding parameters are shown in Table 2. For the specific introduction of the parameters, please refer to [16].

Table 2. GGIW-PHD filter parameters.

Parameter	Value
Birth rate	1×10^{-3}
Death rate	1×10^{-6}
Assignment threshold	220
Extraction threshold	0.8
Confirmation threshold	0.95
Deletion threshold	1×10^{-3}
Labeling threshold	[1.1 1 0.8]
Merging threshold	50

5.2 Experimental Results

A.Selection of Time Threshold

The selection of time threshold is a process that combines experience and mathematical principles. In GW-CATS method, the physical meaning of the time threshold τ is the maximum acceptable time interval between the split target and the original target, and its value is based on the theory of spatio-temporal trajectory similarity: if two trajectories originate from the same target split, their spatio-temporal distribution should maintain continuity in finite time.

Taking the simulation scenario in this section as an example, the speed of the split truck is $25m/s$ and its length is $10m$, then the time required for the target to completely cross its own length is $10 \div 25 = 0.4s$. Considering the geometric uncertainty of the elliptical target after splitting, $\tau = 0.5s$ is finally selected as the equilibrium value. In order to verify the rationality of the threshold, a comparative experiment of $\tau \in [0.1, 1.5]s$ is designed, and the key parameters are set as follows:

- Similarity threshold $\mu = 0.7$.
- Time threshold $\tau = 0.1 - 1.5s$.
- Newborn target validation step $k_{sim} = 4$.

The experiments show that the tracking performance is optimal when $\tau \in [0.4, 0.7]s$. When $\tau < 0.4s$, the real split targets cannot be merged due to the excessively narrow time window, and when $\tau > 0.7s$, adjacent targets are prone to false merging. Under different τ value, the OSPA metric are shown in Figure 5. In what follows, τ of the proposed GW-CATS method is uniformly taken as $0.5s$.

B. Single-Run Results

Figure 4(a) shows the GGIW-PHD tracking results. The detected targets are all represented in the form of elliptical extended targets. It is evident that for target 1 (truck), a distinct segmentation issue occurs after it is obstructed by target 4 (motorcycle), resulting in few false newborn track (target 5-12).

As comparison, Figure 4(b) shows the result with the proposed GW-CATS method. From $k = 71$ to $k = 79$, the truck target split into several false targets. Some of these false targets disappeared during their movement, while others remained until $k = 117$. Taking target 6 generated at k = 72 as an example, after k_{sim} iterations, at $k = 75$, the similarity between new track 6 and tracks 1-4 is $[0.845, 0.629, 0, 0.627]$, so the proposed GW-CATS method decided to fuse target 6 and 1. Further, at $k = 97$ and $k = 117$, the similarity between track 6 and track 1 is 0.896 and 0.910, respectively, so the target fusion process continued, and ultimately the proposed GW-CATS method successfully completed the split determination task. Futhermore, the fusion result is shown in Figure 6.

C.Monte Carlo Results

To evaluate the performance of the GW-CATS method, this section introduces the point-target based CATS method and the global nearest neighbor (GNN)

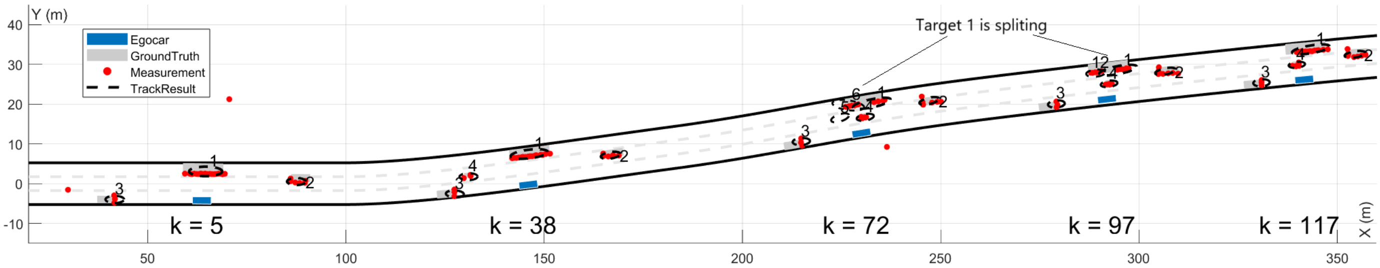

(a) Tracking results of the GGIW-PHD filter.

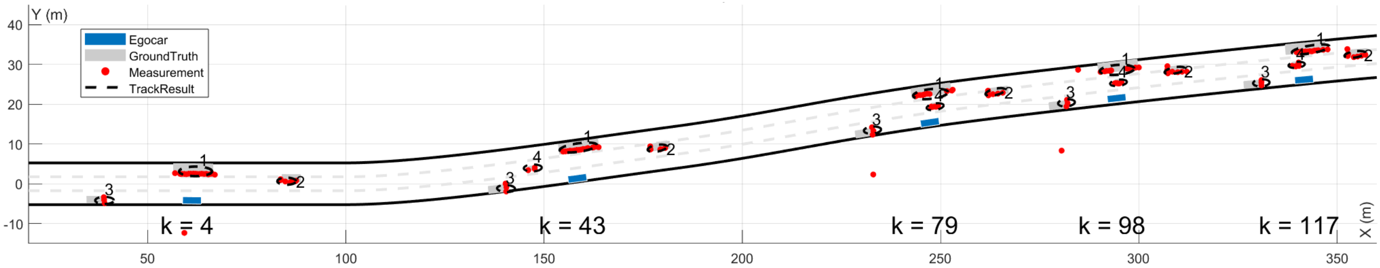

(b) Tracking results of the GGIW-PHD filter corrected by GW-CATS method correction.

Figure 4. Tracking results in single run simulation scenario.

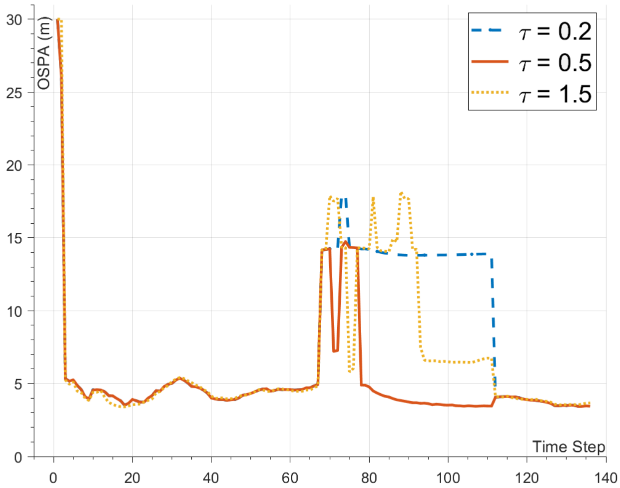

Figure 5. Sensitivity analysis of time threshold for GGIW-PHD filter corrected by GW-CATS method.

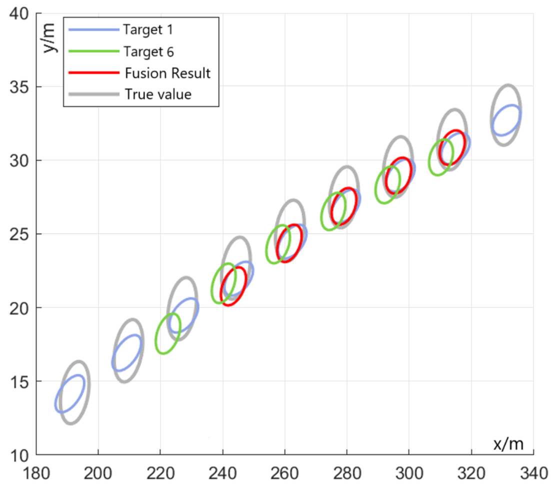

Figure 6. Fusion results. An inner tangent ellipse with the length and width of the rectangle as axes is used to represent the ground truth.

method for comparison with the proposed GW-CATS method. The parameters of the GW-CATS method are consistent with those described in 5.1. The specific parameters of the CATS method are as follows:

- Spatial threshold $\epsilon = 10m$.
- Time threshold $\tau = 0.5s$.

The key parameter configurations of the GNN method are as follows:

- Assignment threshold = 30.
- Detect/Miss Confirmation threshold = [4/5].
- Deletion threshold = 3.

We futher conducted 50 Monte Carlo (MC) trails to demonstrate the effectiveness of the proposed GW-CATS method. The tracking error evaluated by the mean OSPA metric are shown in Figure 7. The tracking error evaluated by the mean GOSPA metric with $p = 1$ and $c = 10m$ are shown in Figure 8.

It can be observed that the OSPA or GOSPA value of the GGIW-PHD filter with GW-CATS correction is greatly reduced when the split target is successfully determined, compared with that of the original GGIW-PHD filter, GNN method and CATS method. It proves that the GW-CATS method can significantly improve the tracking accuracy of extended targets in occlusion scenes.

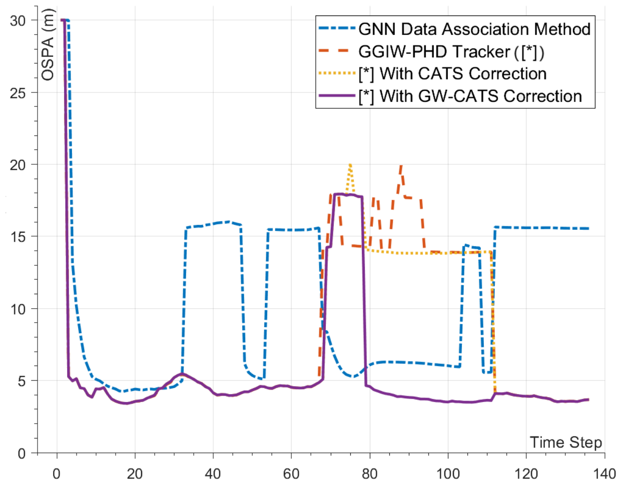

Figure 7. OSPA metric over 50 MC trails, [*] represents the GGIW-PHD Tracker.

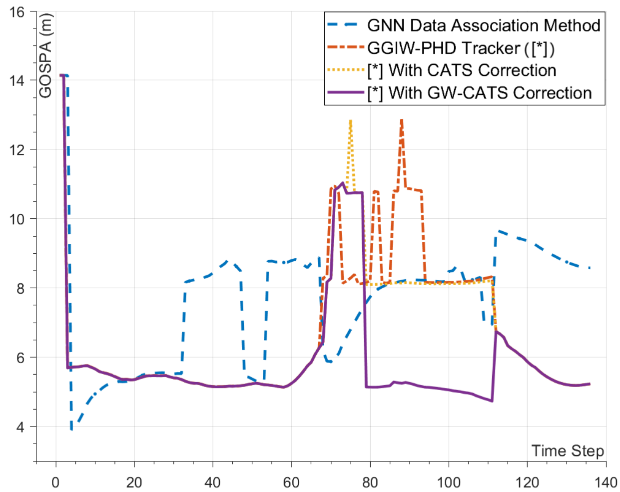

Figure 8. GOSPA metric over 50 MC trails, [*] represents the GGIW-PHD Tracker.

6 Conclusion

To address the splitting correction problem in extended target tracking under occlusion scenarios, we propose a novel track spliting determination method named GW-CATS that integrates the GW distance with spatio-temporal similarity analysis. Simulation results demonstrate that the proposed method can successfully determine the case of target splitting, further reduces the OSPA metric in split scenarios and achieves stable track fusion.

Appendix : The deviation of equation (11)

First, let us set time threshold τ, $p_b^j = (x_0, y_0)$, $p(\tau)_b^j = (x_\tau, y_\tau)$, $v_b^j = (v_x, v_y)$ and turn-rate w_b^j. Then, the direction angle of the velocity vector at the initial time is $\alpha = \arctan(\frac{v_y}{v_x})$, the angle of the target's rotation around the center of the circle is $\theta = \omega_b^j \tau$ and the radius of the arc is $r = \frac{||v_b^j||_2}{|w_b^j|}$. On the one hand, when $w_b^j \neq 0$, it follows that

$$\begin{aligned}
x_\tau &= x_0 + r(\sin(\theta + \alpha) - \sin \alpha) \\
&= x_0 + \frac{1}{|w_b^j|}[\sin(w_b^j t)v_x + \cos(w_b^j t)v_y - v_y] \\
y_\tau &= y_0 + r(-\cos(\theta + \alpha) + \cos \alpha) \\
&= y_0 + \frac{1}{|w_b^j|}[-\cos(w_b^j t)v_x + \sin(w_b^j t)v_y + v_x]
\end{aligned}$$

Then, the Euclidean distance D can be calculated by the following formula

$$\begin{aligned}
D^2 =&(x_\tau - x_0)^2 + (y_\tau - y_0)^2 \\
=&\frac{1}{w_b^{j2}}[(\sin(w_b^j t)v_x + \cos(w_b^j t)v_y - v_y)^2 + \\
&(-\cos(w_b^j t)v_x + \sin(w_b^j t)v_y + v_x)^2] \\
=&\sin^2(w_b^j t)v_x^2 + 2\sin(w_b^j t)\cos(w_b^j t)v_x v_y - \\
&2\sin(w_b^j t)v_x v_y + \cos^2(w_b^j t)v_y^2 - 2\cos(w_b^j t)v_y^2 + v_y^2 + \\
&\cos^2(w_b^j t)v_x^2 2\sin(w_b^j t)\cos(w_b^j t)v_x v_y + 2\cos(w_b^j t)v_x^2 \\
&+ \sin^2(w_b^j t)v_y^2 + 2\sin(w_b^j t)v_x v_y + v_x^2 \\
=&\frac{1}{w_b^{j2}}[2v^2 - 2v^2\cos(w_b^j t)] \\
=&\frac{4v^2}{w_b^{j2}}\sin^2(\frac{w_b^j t}{2})
\end{aligned}$$

Furthermore, on the other hand, when $w_b^j = 0$, the velocity displacement formula can be directly applied for the calculation. Hence, it follows that:

$$D = \begin{cases} \frac{2||v_b^j||_2}{w_b^j}\sin(\frac{w_b^j \tau}{2}), w_b^j \neq 0 \\ ||v_b^j||_2 \times \tau, w_b^j = 0 \end{cases}$$

Data Availability Statement

Data will be made available on request.

Funding

This work was supported in part by the Jiangsu Province Natural Science Foundation of China under Grant BK20230827; in part by the National Natural Science Foundation of China under Grant 62303109; in part by the Zhishan Young Scholar Research Fund of Southeast University under Grant 2242024RCB0011; in part by the Southeast University Start-up Research Fund under Grant RF1028623002.

Conflicts of Interest

The authors declare no conflicts of interest.

Ethical Approval and Consent to Participate

Not applicable.

References

[1] Ersü, C., Petlenkov, E., & Janson, K. (2024). A Systematic Review of Cutting-Edge Radar Technologies: Applications for Unmanned Ground Vehicles (UGVs). *Sensors, 24*(23), 7807. [CrossRef]

[2] Wang, W., Xu, Y., Zhang, K., Sun, Y., & Li, P. (2025). A GGIW PMBM Smoother for Multiple Extended Object Tracking. *Electronics Letters, 61*(1), 1-5. [CrossRef]

[3] Yang, C., Cao, X., & Shi, Z. (2023). Road-map aided Gaussian mixture labeled multi-Bernoulli filter for ground multi-target tracking. *IEEE Transactions on Vehicular Technology, 72*(6), 7137-7147. [CrossRef]

[4] Granstrom, K., Lundquist, C., & Orguner, O. (2012). Extended target tracking using a Gaussian-mixture PHD filter. *IEEE Transactions on Aerospace and Electronic Systems, 48*(4), 3268-3286. [CrossRef]

[5] Granstrom, K., & Orguner, U. (2012). A PHD filter for tracking multiple extended targets using random matrices. *IEEE Transactions on Signal Processing, 60*(11), 5657-5671. [CrossRef]

[6] Habtemariam, B., Tharmarasa, R., Thayaparan, T., Mallick, M., & Kirubarajan, T. (2013). A multiple-detection joint probabilistic data association filter. *IEEE Journal of Selected Topics in Signal Processing, 7*(3), 461-471. [CrossRef]

[7] Zhang, G., Lian, F., & Han, C. (2014). CBMeMBer filters for nonstandard targets, I: extended targets. In *17th International Conference on Information Fusion* (pp. 1-6).

[8] Beard, M., Reuter, S., Granström, K., Vo, B. T., Vo, B. N., & Scheel, A. (2015). Multiple extended target tracking with labeled random finite sets. *IEEE Transactions on Signal Processing, 64*(7), 1638-1653. [CrossRef]

[9] Granström, K., Fatemi, M., & Svensson, L. (2016). Gamma Gaussian inverse-Wishart Poisson multi-Bernoulli filter for extended target tracking. In *19th International Conference on Information Fusion* (pp. 893-900).

[10] Xu, M., Yang, C., Cao, X., Yang, S., Cao, X., & Shi, Z. (2024). Irregular extended target tracking with unknown measurement noise covariance. *Signal Processing, 225*, 109600. [CrossRef]

[11] Wang, G., Wang, Y., Gu, R., Hu, W., & Hwang, J. N. (2022). Split and connect: A universal tracklet booster for multi-object tracking. *IEEE Transactions on Multimedia, 25*, 1256-1268. [CrossRef]

[12] Asad, M., Khan, S., Mehmood, Z., Shi, Y., Memon, S. A., & Khan, U. (2020). A split target detection and tracking algorithm for ballistic missile tracking during the re-entry phase. *Defence Technology, 16*(6), 1142-1150. [CrossRef]

[13] Jin, J., Ma, M., & Liu, C. (2021, December). Group Targets Splitting Algorithm for Ballistic Missile Penetration Applications. In *2021 CIE International Conference on Radar* (*Radar*) (pp. 843-847). IEEE. [CrossRef]

[14] Dong, L., Zhang, Y., Zhao, L., Zheng, T., Wang, W., Li, J., ... & Yao, D. (2022). DRT: A new toolbox for the Standard EEG Data Structure in large-scale EEG applications. *SoftwareX, 17*, 100933. [CrossRef]

[15] Yang, C., Liang, X., Shi, Z., Zhang, H., & Cao, X. (2025). Augmented LRFS-based filter: Holistic tracking of group objects. *Signal Processing, 226*, 1-10. [CrossRef]

[16] Granström, K., Natale, A., Braca, P., Ludeno, G., & Serafino, F. (2015). Gamma Gaussian inverse Wishart probability hypothesis density for extended target tracking using X-band marine radar data. *IEEE Transactions on Geoscience and Remote Sensing, 53*(12), 6617-6631. [CrossRef]

[17] Yang, S., Baum, M., & Granström, K. (2016). Metrics for performance evaluation of elliptic extended object tracking methods. In *IEEE International Conference on Multisensor Fusion and Integration for Intelligent Systems* (pp. 523-528). [CrossRef]

[18] Loraamm, R., Downs, J., Anderson, J., & Lamb, D. S. (2020). PySTPrism: Tools for voxel-based space–time prisms. *SoftwareX, 12*, 1-5. [CrossRef]

[19] Zheng, Y. (2015). Trajectory data mining: an overview. *ACM Transactions on Intelligent Systems and Technology, 6*(3), 1-41. [CrossRef]

[20] Sun, L., & Zhou, W. (2017). A multi-source trajectory correlation algorithm based on spatial-temporal similarity. In *20th International Conference on Information Fusion* (pp. 1-7). [CrossRef]

[21] Thormann, K., & Baum, M. (2019). Optimal fusion of elliptic extended target estimates based on the Wasserstein distance. In *22th International Conference on Information Fusion* (pp. 1-6). [CrossRef]

[22] Schuhmacher, D. , Vo, B. T. , & Vo, B. N.(2008). A consistent metric for performance evaluation of multi-object filters.*IEEE Transactions on Signal Processing, 56*(8), 3447-3457. [CrossRef]

[23] Rahmathullah, A. S. , García-Fernández, Ángel F, & Svensson, L.(2016). Generalized optimal sub-pattern assignment metric. In *20th International Conference on Information Fusion* (pp. 1-8). [CrossRef]

Jiashi Shen received the B.Eng. degree in Automation from Nanjing University of Science and Technology, Nanjing, China, in 2024. He is currently working toward the M.Eng. degree in Control Engineering with the School of Automation, Southeast University, Nanjing, China. His research interest concentrates on extend target tracking, neural network tracking and information fusion.

Chaoqun Yang received the B.Sc. degree in marine technology from Xiamen University, Xiamen, China, in 2014, and the Ph.D. degree in information science and electronic engineering from Zhejiang University, Hangzhou, China, in 2019. From 2019 to 2022, he was an Engineer with the Nanjing Research Institute of Electronics Technology, Nanjing, China. Since 2022, he has been an Associate Professor with the School of Automation, Southeast University, Nanjing. His research interest concentrates on multitarget tracking, radar signal processing, cyber security, and information fusion. Dr. Yang was the Session Co-Chair of *IEEE/CIC ICCC2024*, *ICSPS2024*, and *ICAUS2024*, and received the Best Paper Award of *ICAUS2024*.

Lidong He received the B.Eng. degree in mechanical engineering from Zhejiang Ocean University, Zhoushan, China, in 2005, the master's degree in control theory and control engineering from Northeastern University, Shenyang, China, in 2008, and the Ph.D. degree in control science and engineering from Shanghai Jiao Tong University, Shanghai, China, in 2014.

In the fall of 2010 and 2011, he was a visiting student with The Hong Kong University of Science and Technology, Hong Kong. From 2014 to 2016, He was a Postdoctoral Researcher with Zhejiang University, Hangzhou, China. In 2016, He joined the School of Automation, Nanjing University of Science and Technology, Nanjing, China, and is currently an Associate Professor. His research interests include secure estimation and control for cyber physical systems and its application in unmanned systems.

Dr. He is an active reviewer for many international journals.

Xianghui Cao received the B.S. and Ph.D. degrees in control science and engineering from Zhejiang University, Hangzhou, China, in 2006 and 2011, respectively.

From 2012 to 2015, he was a Senior Research Associate with the Department of Electrical and Computer Engineering, Illinois Institute of Technology, Chicago, IL, USA. He is currently a Professor with the School of Automation, Southeast University, Nanjing, China. His current research interests include cyber–physical' systems, wireless network performance analysis, wireless networked control, and network security.

Prof. Cao was a recipient of the Best Paper Runner-Up Award from ACM MobiHoc in 2014 and the First Prize of Natural Science Award of Ministry of Education of China in 2017. He also serves as an Associate Editor for *ACTA Automatica Sinica* and IEEE/CAA *JOURNAL OF AUTOMATICA SINICA*.